Preparation of Ti–Al and Fe–Al Alloys by Mechanical Alloying

A. Bernatiková, P. Novák* and F. Průša

University of Chemistry and Technology Prague, Department of Metals and Corrosion Engineering,
Technická 5, 166 28 Prague 6, Czech Republic

This work aims to describe the formation of intermetallics in Ti–Al and Fe–Al systems during ultra-high energy mechanical alloying process developed by authors. Although both systems tend to form aluminides, the formation of the phases during mechanical alloying is different. It was found that TiAl38 (in wt.%) powder mixture forms dual-phase TiAl/Ti$_3$Al structure, which is consequently transformed to almost single-phase TiAl structure as the duration of mechanical alloying increases. On the other hand, FeAl32 (in wt.%) powder mixture formed ordered FeAl phase in the early steps, which was consequently changed to disordered solid solution after longer milling.

1. Introduction

Ti–Al system contains four stable intermetallic phases — Ti$_3$Al, TiAl, TiAl$_2$ and Ti$_3$Al. First of them, Ti$_3$Al ($\alpha2$) is characterized by aluminium content ranging between 22 at.% and 39 at.%. This phase has the hexagonal $D0_{19}$ ($P6_3/mmc$) structure. The lattice parameters of the phase are $a = 5.77 \times 10^{-10}$ m and $c = 4.62 \times 10^{-10}$ m. Second one, TiAl, also called γ phase, contains 48.5 at.% to 66 at.% of aluminium. Crystal structure of this phase is of the tetragonal $L1$ type ($P4/mmm$) with the lattice parameters of $a = 3.98 \times 10^{-10}$ m and $c = 4.07 \times 10^{-10}$ m [1, 2]. Both the above-mentioned phases are of the highest technical importance among the Ti–Al phases due to their good mechanical properties at high temperatures. The highest operation temperature of the Ti$_3$Al phase is usually declared as 650 °C and 760 °C in air (oxidation limit) and inert atmosphere (creep limit), respectively. In the case of TiAl phase, the oxidation limit is 900 °C and creep limit reaches the value of 1000 °C. In technical materials, these phases are usually combined, having the aluminium content ranging between 37 to 49 at.%. Structure of this material is composed of lamellae of Ti–Al and Ti$_3$Al phases, resulting in improved toughness of the alloy. This kind of alloy is currently applied in modern jet engines of airplanes or turbocharger wheels of car combustion engines [3]. In addition to these phases, there are also TiAl$_2$ and TiAl$_3$ phases in the Ti–Al system. However, these intermetallics are much more brittle than the TiAl/Ti$_3$Al phases and hence they are not technically applicable. TiAl$_2$ phase is body centered tetragonal ($I4_1/amd$) with lattice parameters $a = 3.97 \times 10^{-10}$ m and $c = 24.30 \times 10^{-10}$ m. The structure of TiAl$_3$ phase is $D0_{22}$ ($I4/mmm$) with lattice parameters of $a = 3.84 \times 10^{-10}$ m and $c = 8.58 \times 10^{-10}$ m [1, 2].

The stable binary Fe–Al intermetallic phases are Fe$_3$Al with cubic $D0_3$ structure ($Fm\bar{3}m$ space group, $a = 5.8 \times 10^{-10}$ m, Al content from 23 to 34 at.%), FeAl (cubic $B2$ structure, $Pm\bar{3}m$, $a = 2.8954 \times 10^{-10}$ m, Al content from 23.3 to 55 at.%), FeAl$_2$ (triclinic $P1$, $a = 4.8745 \times 10^{-10}$ m, $b = 6.4545 \times 10^{-10}$ m, $c = 8.7361 \times 10^{-10}$ m, $\alpha = 87.93°$, $\beta = 74.396°$, $\gamma = 83.062°$, Al content 66–69.9 at.%), Fe$_2$Al$_5$ (orthorhombic $Cmcm$, $a = 7.6750 \times 10^{-10}$ m, $b = 6.4030 \times 10^{-10}$ m, $c = 4.2030 \times 10^{-10}$ m, 70–73 at.% Al) and FeAl$_3$, also denoted as Fe$_4$Al$_{13}$ (monoclinic $C2/m$, $a = 15.489 \times 10^{-10}$ m , $b = 8.083 \times 10^{-10}$ m, $c = 12.476 \times 10^{-10}$ m, $\beta = 107.69°$, 74.5–76.6 at.% Al) [1, 2, 4]. Among these phases, FeAl and Fe$_3$Al are of the highest interest due to acceptable fracture toughness at room temperature and good mechanical properties at high temperatures (up to approximately 600 °C) [5]. Fe–Al based alloys also have excellent resistance against high-temperature oxidation and sulphidation and therefore the application range can cover e.g. power engineering, furnace elements, exhaust valves of combustion engines and also specific areas in chemical industry [5]. However, wider utilization of both Fe–Al and Ti–Al alloys is limited by the manufacturing problems in conventional melting metallurgy, caused by poor castability, susceptibility to hot cracking and high reactivity of the melts, especially in the case of titanium-based intermetallics [6]. These problems could be possibly overcome by employing the powder metallurgy process.

Among the powder metallurgy techniques, mechanical alloying combined with advanced consolidation methods seem to be highly promising. Mechanical alloying is in fact a high energy milling process, which comprises cold welding of particles, fracturing due to deformation strengthening and formation of compounds by thermally activated reactions supported by friction and transformation of the kinetic energy of the milling medium, usually balls [7]. The intermetallics are usually obtained in 20–100 h of milling or after milling and subsequent

————

*corresponding author; e-mail: panovak@vscht.cz

annealing in the studied systems. Even the FeAl TiAl composites reinforced with ceramic particles (e.g. Y_2O_3 or TiC) were already prepared [8, 9]. Some attempts were done to shorten the duration of mechanical alloying, e.g. the milling of TiH2 and TiAl3 phases [10] or dual phase mechanical alloying with the intermediate annealing step (i.e. milling–annealing–milling) [11]. The authors previously developed the simple and efficient modification of the mechanical alloying — ultra-high energy mechanical alloying [12]. In this technology, the intermetallics can be yielded in 1–4 h due to complex optimization of the process (ball-to-powder ratio, rotational velocity) and absence of any process control agents or lubricants [12]. This work aims to describe the formation of Ti–Al and Fe–Al intermetallics during this quick and innovative process.

2. Experimental

Powders of TiAl38 (wt.%) and FeAl32 (wt.%) were prepared by blending of the appropriate amounts of iron powder (purity 99.9 wt.%, particle size $< 44\ \mu$m, supplied by Sigma Aldrich), aluminium powder (purity 99.7 wt.%, particle size $< 44\ \mu$m, supplied by Alfa Aesar) and titanium powder (purity 99.99 wt.%, particle size $< 44\ \mu$m, supplied by Alfa Aesar). Prepared powder mixtures were mechanically alloyed in a planetary ball mill (Retsch PM 100 CM). Milling vessel and the milling balls were both made of AISI 420 stainless steel. The overall parameters of mechanical alloying are following: rotational velocity of 400 rpm, milling duration 1–8 h, argon atmosphere, powder batch 5 g, ball-to-powder ratio of 64:1.

Phase composition was evaluated by X-ray diffraction (PANalytical X'Pert Pro with Cu K_α radiation). The obtained XRD patterns were processed qualitatively using the HighScore Plus software package and reference PDF2 database.

The metallographic samples were prepared by embedding of the powders into the epoxy resin. Then samples were ground by the use of grinding papers with SiC abrasive particles (P400-P2500), polished by a diamond paste D2 and consequently by a suspension composed of colloidal silica (Eposil F) mixed with hydrogen peroxide (mixed in ratio of 1:1). Samples were etched by modified Kroll's reagent (2 ml HNO_3, 6 ml HF, 92 ml H_2O). The microstructure of the powders was studied by the means of scanning electron microscopy (SEM, TESCAN VEGA 3 LMU) equipped with energy dispersive X-ray spectrometer (EDS, Oxford Instruments X-max 20 mm² SDD analyzer).

3. Results and discussion

3.1. Ti–Al

Mechanical alloying of TiAl38 powder for 1 h results in a dual-phase microstructure composed of Ti_3Al and TiAl phases (Fig. 1). The same composition was seen also after 2 h milling. Microstructure of powders mechan-

ically alloyed for 1 h showed that the dual-phase structure is composed of TiAl (dark grey) and Ti_3Al (light grey) lamellae (Fig. 2a). Powder mechanically alloyed for 2 h possesses the same phase composition, but completely different morphology of the phases, see Fig. 2b. There are coarser regions of the TiAl and Ti_3Al phases.
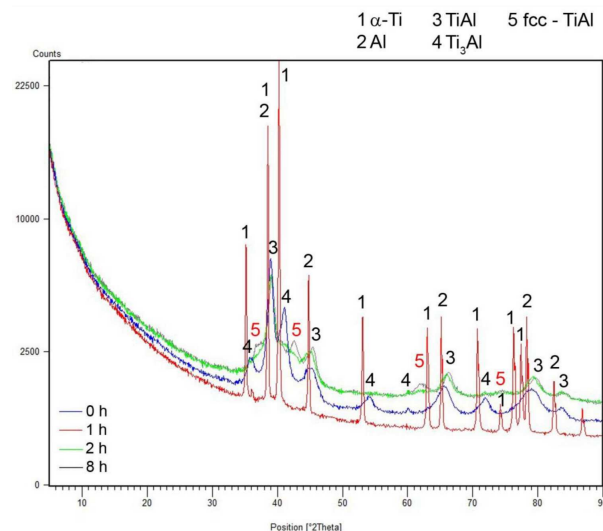

Fig. 1. XRD patterns of TiAl38 (in wt.%) powder mixture after various durations of mechanical alloying.

After longer milling times (3 h and more), only the TiAl phase has been detected (Fig. 1). The TiAl38 powder prepared by 3 h of mechanical alloying was nearly homogeneous TiAl phase, which was partially contaminated by iron (white particles in Fig. 2c). Contamination was probably caused by the wear of the milling vessel and balls during the process. There are also small localized regions of residual Ti_3Al phase (Fig. 2c).

During the next stage of mechanical alloying, new peak appeared in the XRD pattern. According to [13], these peaks belong to the fcc TiAl disordered solid solution. It should be also noted the peaks broadening occurred with the prolongation of the mechanical alloying process suggesting microstructural refinement and also accumulation of the internal stress in the lattice. The microstructure was almost homogeneous TiAl phase (Fig. 2d), containing minor traces of contamination by iron (white particles) and other fine particles, being probably the above mentioned fcc TiAl disordered solid solution. EDS analysis results, which helped to recognize individual TiAl phases on SEM micrographs, are shown for illustration in Table I.

TABLE I

Average composition of the phases in TiAl38 powder mixtures after mechanical alloying (determined by EDS)

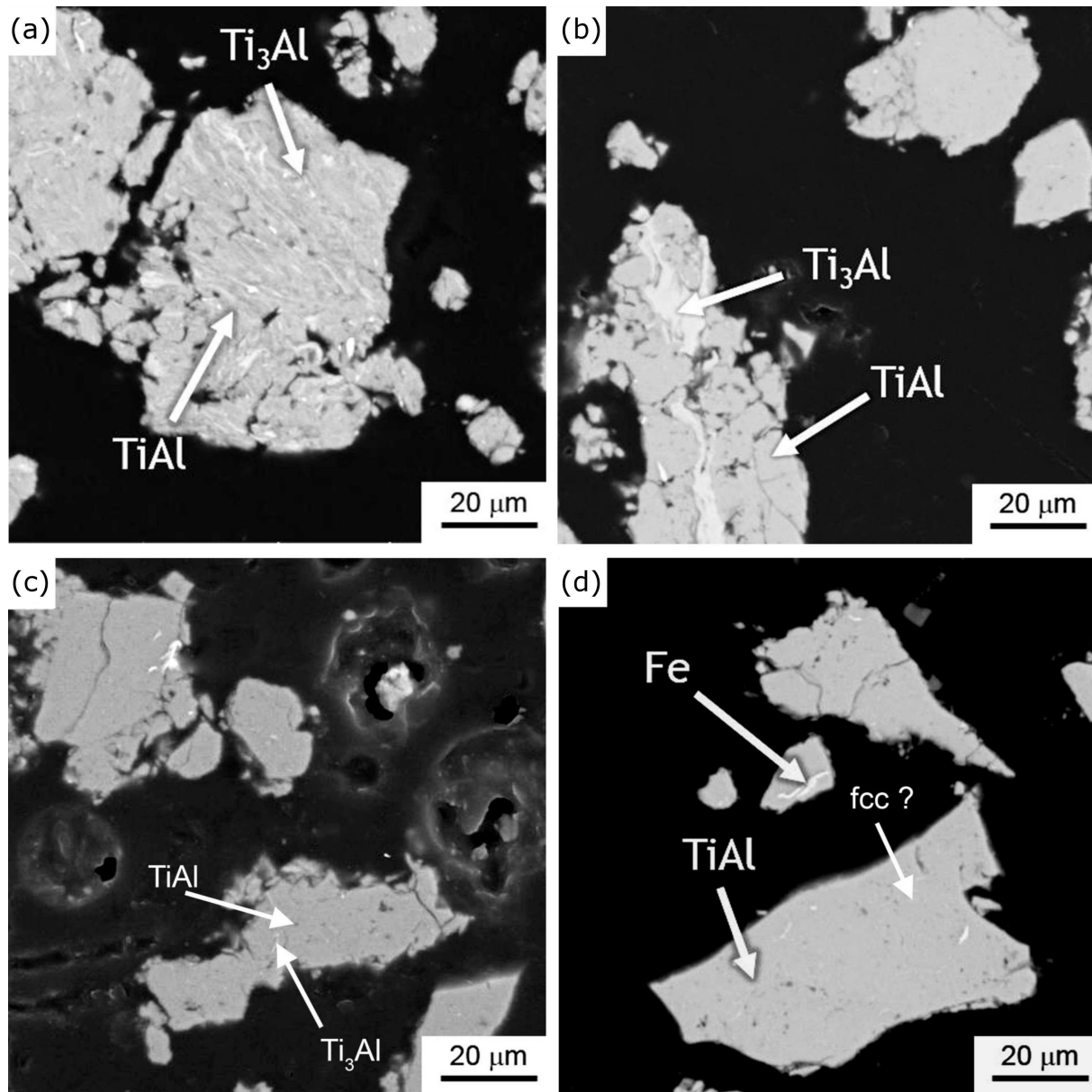| Phase	Ti [at.%]	Al [at.%]
TiAl	42 ± 2	53 ± 2
Ti_3Al	77 ± 4	23 ± 4
fcc –TiAl (?)	49 ± 3	51 ± 3

Fig. 2. Microstructure of TiAl38 (in wt.%) powder mixture mechanically alloyed for: (a) 1 h, (b) 2 h, (c) 3 h, (d) 8 h.

3.2. Fe–Al

Diffraction patterns of the FeAl32 powder mixture after various durations of mechanical alloying are presented in Fig. 2. EDS analysis results, which helped to recognize individual Fe–Al phases on SEM micrographs, are shown for illustration in Table II. It is obvious that iron aluminides behaved differently than the titanium aluminides. After 1 h of mechanical alloying, the presence of unreacted iron and aluminium was proved by XRD. Microstructure of FeAl32 powder mechanically alloyed for 1 h contained light particles corresponding to the unreacted iron, dark particles of unreacted aluminium and grey particles FeAl phase (Fig. 3a).

According to the XRD results, nearly single-phase FeAl structure was achieved after milling for 2 h, containing minor admixture of $FeAl_3$ phase. Formation of FeAl phase is confirmed mostly by the presence of a peak at $30.819°$, associated with the (100) plane of the FeAl ordered phase ($B2$ structure type). When comparing the results with recent paper by Shi et al. [14], who observed a formation of the single-phased FeAl structure after mechanical alloying for more than 30 h, one can see that our optimized ultra-high energy process enables to yield intermetallics in really short process duration. However, there were regions of unreacted iron (Fig. 3b) also found in the structure during SEM observation and EDS analysis. The discrepancy between XRD and SEM-EDS results is probably caused by the fact that the α-Fe diffraction lines are in overlap with $B2$ FeAl phase due to saturation by aluminium (Fig. 4, Table II).
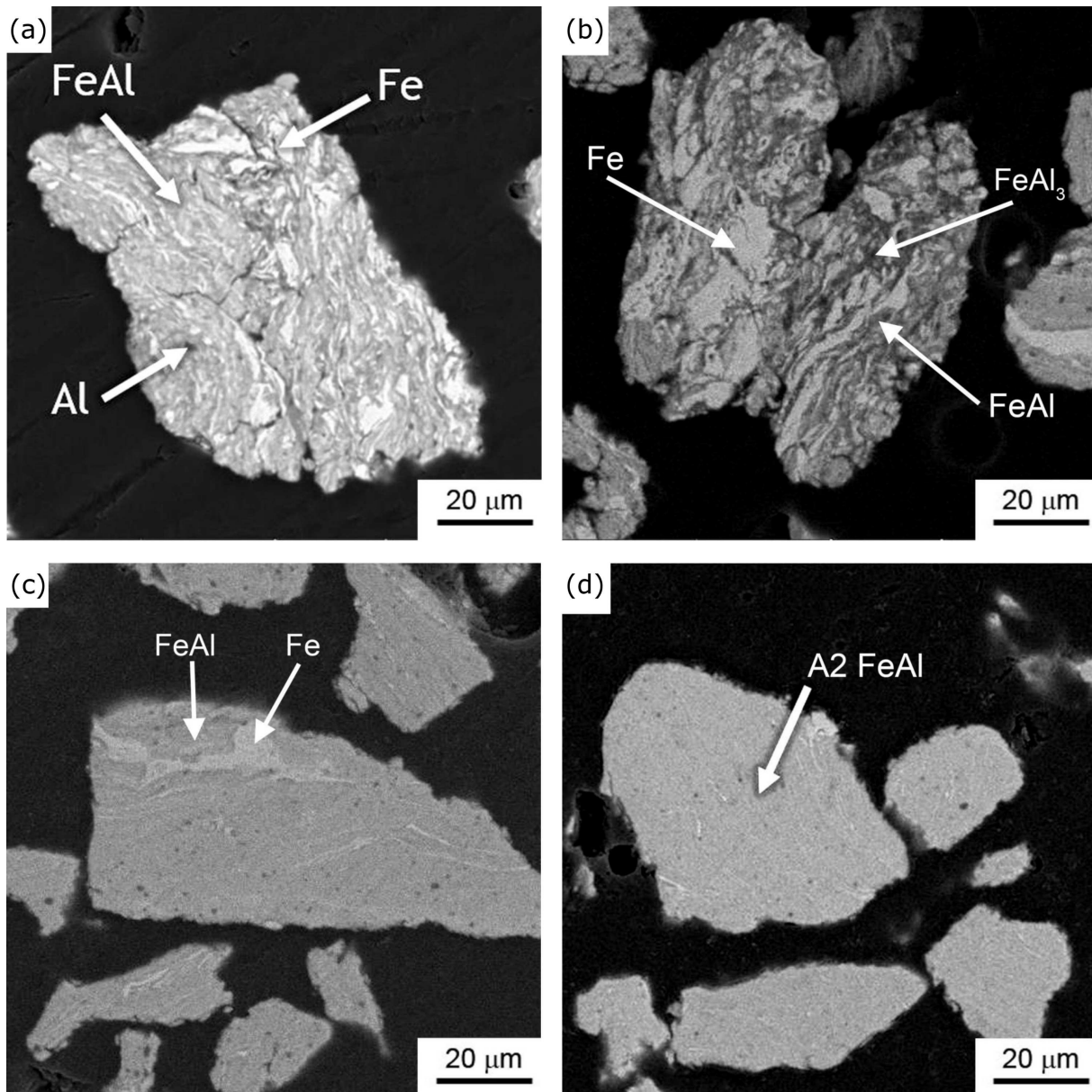
Fig. 3.   Microstructure of FeAl32 (in wt.%) powder mixture mechanically alloyed for: (a) 1 h, (b) 2 h, (c) 3 h, (d) 8 h.

The ordering to FeAl phase with $B2$ structure was observed without the Fe_2Al_5 intermediate phase, which has been detected previously in reactive sintering synthesis of the FeAl phase. The minor amount of $FeAl_3$ formed after 2 h of milling, but after the FeAl phase arose. The difference between the mechanism of reactive sintering and mechanical alloying is probably caused by two effects: in reactive sintering, significant part of the reaction proceeds on the interface between molten aluminium and solid iron [15]. On the other hand, in mechanical alloying the processes highly probably proceed under the melting point of aluminium. Second factor, which probably plays a role, is the mechanical deformation, which introduces high number of crystal defects to the material. It implies that ordering could proceed more easily.

TABLE II

Average composition of the phases in FeAl32 powder mixtures after mechanical alloying (determined by EDS)

Phase	Fe [at.%]	Al [at.%]
Fe	96 ± 4	4 ± 4
B2 FeAl	52 ± 6	48 ± 6
FeAl$_3$	77 ± 3	23 ± 3
A2 FeAl	51 ± 5	49 ± 5

After 8 h of mechanical alloying, the peak positions fit to the FeAl phase. However, the characteristic peak of $B2$ FeAl phase at 30.819° is missing. It shows that the $B2$ ordered phase was converted to disordered FeAl solid solution with $A2$ structure. This phenomenon has been already described in literature, but after much longer pro-

cess duration [16]. The milling duration of 8 h resulted in homogeneous structure (Fig. 4c) of a chemical composition (determined by EDS) corresponding to the FeAl phase. It confirms well the results of the XRD analysis, which detected the disordered (A2) FeAl phase.
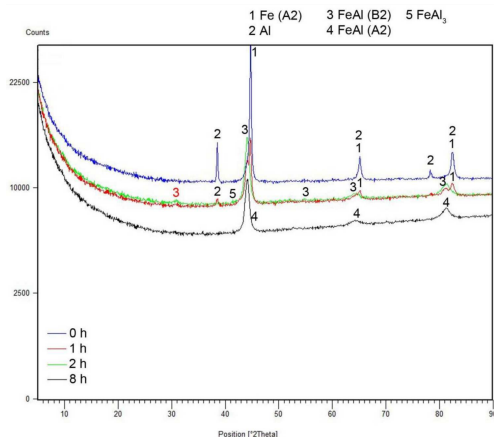

Fig. 4. RD patterns of FeAl32 (in wt.%) powder mixture after various durations of mechanical alloying.

4. Discussion

The mechanisms of mechanical alloying in relevant literature are presented differently. In Ti–Al system, of the preference is formation of solid solution, which amorphizes and crystallizes again in different structure. This behaviour can be seen in the work by Suryanarayana et al. [13]. In contrast to our results, the products of milling were composed of Ti–Al solid solution only, when comparable milling duration (3 h) was applied. Prolongation of mechanical alloying caused the amorphization of the phase and subsequent crystallization of the fcc phase after 11 to 36 h. Other authors proved the formation of Ti50Al50 (at.%) hcp phase after milling under different conditions. This phase was then converted to tetragonal γ-TiAl by annealing [17].

In Fe–Al powders of various compositions, only minor amount of Fe_3Al phase was formed after long durations of conventional mechanical alloying [18]. The refined structure of lamellae of iron and aluminium obtained by this process was able to be converted to Fe–Al phases by subsequent annealing.

It suggests that our highly energetic process in fact combines the conventional mechanical alloying and annealing, because the heat is generated by friction between balls and milling vessel in the absence of lubricant. This heat is dissipated and it increases local temperature of the powder and initiates the formation of intermetallics. Therefore, the mechanism of our ultra-high energy mechanical alloying is closer to the self-propagating high-temperature synthesis (SHS) than to conventional mechanical alloying in both of the studied systems [19].

5. Conclusions

The results of this study showed dissimilarity in the mechanical alloying behaviour of the investigated TiAl38

and FeAl32 (in wt.%) powder mixtures. It was found that the mixture based on titanium forms firstly the dual-phase structure composed of TiAl and Ti_3Al structures and as the alloying time prolongs it tends to form only single-phase TiAl structure. On the other hand, the FeAl38 powder mixture forms B2 FeAl structure directly from iron and aluminium powder. The minor amount of $FeAl_3$ phase was formed, but after longer milling than B2 FeAl phase appeared. The B2 FeAl then transforms to the disordered solid solution (A2 FeAl), as the milling continues.

References

[1] T.B. Massalski, *Binary Alloy Phase Diagrams*, ASM, Materials Park 1990.

[2] International Centre for Diffraction Data, *PDF-4+ 2010* (Database), Ed. Soorya Kabekkodu, Newtown Square (PA), USA.

[3] K. Kothari, R. Radhakrishnan, N.M. Wereley, *Progr. Aero. Sci.* **55**, 1 (2012).

[4] X. Li, A. Scherf, M. Heilmaier, F. Stein, *J. Phase Equilib. Diff.* **37**, 162 (2016).

[5] D.G. Morris, M.A. Muńoz-Morris, *Adv. Eng. Mater.* **13**, 43 (2011).

[6] J. Barbosa, C. Silva Ribeiro, A. Caetano Monteiro, *Intermetallics* **15**, 945 (2007).

[7] F.H. Froes, C. Suryanarayan, K. Russell, C. Li, *Mater. Sci. Eng. A* **192**/**193**, 612 (1995).

[8] J.H. Schneibel, P. Grahle, J. Rösler, *Mater. Sci. Eng. A* **153**, 684 (1992).

[9] M. Zakeri, M.R. Rahimipour, *Powder Metall.* **54**, 278 (2011).

[10] C. Suryanarayana, R. Sundaresan, F.H. Froes, *Mater. Sci. Eng. A* **150**, 117 (1992).

[11] S. Xiao, L. Xu, Y. Chen, H. Yu, *Trans. Nonferrous Met. Soc. China* **22**, 1086 (2012).

[12] P. Novák, T. Kubatík, J. Vystrčil, R. Hendrych, J. Kříž, J. Mlynár, D. Vojtěch, *Intermetallics* **52**, 131 (2014).

[13] C. Suryanarayana, G.-H. Chen, A. Frefer, F.H. Froes, *Mater. Sci. Eng. A* **158**, 93 (1992).

[14] H. Shi, D. Guo, Y. Ouyang, *J. Alloys Comp.* **455**, 207 (2008).

[15] P. Novák, A. Michalcová, I. Marek, M. Mudrová, K. Saksl, J. Bednarčík, P. Zikmund, D. Vojtěch, *Intermetallics* **32**, 127 (2013).

[16] L.S.J. Peng, G.S. Collins, *Mater. Sci. Forum* **235-238**, 537 (1997).

[17] K.B. Gerasimov, S.V. Pavlov, *J. Alloys Comp.* **242**, 136 (1996).

[18] M.H. Enayati, M. Salehi, *J. Mater. Sci.* **40**, 3933 (2005).

[19] P. Novák, J. Šerák, A. Michalcová, J. Kubásek, D. Vojtěch, *Int. J. Mater. Res.* **100**, 353 (2009).